Vietnam Journal of Catalysis and Adsorption
Tạp chí xúc tác và hấp phụ Việt Nam

https://chemeng.hust.edu.vn/jca/

Mechanical and weather resistance improvement of polyurethane thin films embedded with nanocomposites CeO_2-SiO_2

Nguyen Quang Bac[1,2,*], Nguyen Thi Ha Chi[2], Doan Trung Dung[2], Pham Ngoc Chuc[2], Duong Thi Lim[3], Dao Ngoc Nhiem[1,2], Tran Dai Lam[4]

[1] Graduate University of Science and Technology, Vietnam Academy of Science and Technology, 18 Hoang Quoc Viet, Hanoi, Viet Nam
[2] Institute of Materials Science, Vietnam Academy of Science and Technology, 18 Hoang Quoc Viet, Hanoi, Viet Nam
[3] Institute of Geography, Vietnam Academy of Science and Technology, 18 Hoang Quoc Viet, Hanoi, Viet Nam
[4] Institute for Tropical Technology, Vietnam Academy of Science and Technology, 18 Hoang Quoc Viet, Hanoi, Viet Nam
**Email: quangbac1993@gmail.com*

ARTICLE INFO

Received: 15/5/2021
Accepted: 15/7/2021
Published: 15/10/2021

Keywords:

Polyurethane, weather resistance, CeO_2-SiO_2, nanocomposites, thin film

ABSTRACT

Polyurethane (PU) thin films quickly degrade under the presence of oxygen, vapor, temperature, and ultraviolet irradiation. Thus, efforts have been dedicated to improving the properties of PU films. This study presents a simple synthesis route to prepare PU embedded with CeO_2-SiO_2 nanocomposites (CS NCs). At first, the CS NCs were synthesized by a gel combustion method using polyvinyl alcohol. Prepared nanocomposites were characterized by X-ray diffraction spectrometry, scanning electron microscopy. Next, the prepared nanocomposites were filled into PU films with the loading from 0.1 % and 2.0 % wt. The mechanical properties of these films were evaluated following the DIN standards. Furthermore, these films also were subjected to a QUV accelerated weathering test to investigate the weather resistance capacity.

Introduction

Polyurethane (PU) films occur in many fields such as transportation, furniture, automotive, and textile industries [1,2]. However, when exposed to an environment where oxygen, water, pollutant, and sunlight presences, coating films are affected and gradually degraded. As a result, the mechanical properties of the films reduce rapidly [3]. Briefly, direct sunlight reduces cohesion between substances as well as color, the gloss of the films after a short period of use. It can be understood that UV irradiations are the leading cause of film degradation, which can break organic structures [3,4], causing film aging and discoloration.

In order to limit the impact of UV irradiation on the film, some active substances have been added, such as CeO_2, ZnO, TiO_2, Fe_2O_3, or graphene [5-12]. However, single materials often show disadvantages such as limited adsorption capacity, high agglomeration, and unstable at elevated temperature. Therefore, nanocomposites that can exhibit the synergy effect of different materials are potential candidates [5,13–17]. Among them, CeO_2-SiO_2 nanocomposites (CS NCs) show an excellent optical property and high stability. Due to the small size of CeO_2-SiO_2 nanocomposites

https://doi.org/10.51316/jca.2021.117

(i.e., < 50 nm), [18,19] the bonding force between them significantly affects their separation when dispersed in the film matrix. The ability to disperse materials into the film will determine the improved efficiency of the material. When CS NCs are not distributed properly, it even decreases the mechanical properties of the coatings.

Herein, this study utilizes a gel combustion method using polyvinyl alcohol (PVA) to synthesize CS NCs followed a relatively simple route. Then, the prepared nanocomposites were dispersed into PU matrix formed functional films using a grinding method, which can apply in various fields such as the automotive industry, wood industry, or food industry. Besides being exposed to 700 h of accelerated artificial weather, mechanical properties of the prepared polymer film were examined following DIN standards (for examples, DIN 50324, DIN 53152). The bonding configuration of the coating was investigated using FTIR spectroscopy. This strategy offers a promising application such as coatings for automobiles and other industries such as furniture and wood.

Experimental

Chemicals

All reagents for preparing CS NCs were used without any further purification, including $Si(OC_2H_5)_4$ (TEOS, 99 %, Sigma Aldrich), $Ce(NO_3)_3.6H_2O$ (99 %, Sigma Aldrich), poly(vinyl alcohol) (PVA, 99 %, Sigma Aldrich), 30 % NH_4OH solution (Sigma Aldrich) and CH_3COOH (99 %, Sigma Aldrich).

Chemicals employed for preparing polyurethane films were obtained in industrial qualities, including a diisocyanate (Desmodur® Z 4470 MPA/X, BASF Vietnam), two acrylic polyols (Acrydic AC-3252 and Olester AO-529, TOP solvent), and other organic solvents (TOP solvent).

PVA (99%, Sigma Aldrich) was preferred to use in this study because of its superior properties such as inexpensive, biodegradable, non-toxic materials. Besides, PVA helps the homogeneous distribution of the metal ions and inhibits their segregation/precipitation from the solution [20,21]. Furthermore, PVA was also selected as a complexing agent that reduces the agglomeration effect of metal ions.

CS NCs preparation

In this study, the nanocomposites were prepared from a simple route which was detailly described in our previous paper [14]. Briefly, 0.434 g of $Ce(NO_3)_3.6H_2O$ and 0.208 g of $Si(OC_2H_5)_4$ (1:1 molar ratio) were added to 55.8 ml of 5.0 % PVA solution. The pH level was adjusted to 4.0 by adding 1M CH_3COOH and 30 % NH_4OH solutions. The mixture was stirred at 80 °C for 4 hours until a homogeneous gel was formed. The gel was dried at 105 °C for 8 hours before being calcinated at 650 °C for 2 hours.

Polyurethane films preparation

Weigh a proportional amount of the synthesized CS NCs, then thoroughly dispersed into a mixture of acrylic polyols, solvents, and additives, grinding for four hours. When the mixture turned into a suspension, it was filtered through a 37-mm filter and adjusted with solvents to have a 100 g mixture. The amount of CS NCs was prepared so that the final content varied from 0.1 wt% to 2 wt% (i.e., 0.1 wt%, 0.25 wt%, 0.5 wt%, 1.0 wt%, 1.5 wt%, 2.0 wt%). Next, isocyanate and a mix of solvents were added, followed by stirring until a homogenous mixture with a viscosity of 12.5 m^2.s was obtained. The mixture was sprayed onto ABS panels using an automotive paint gun, aged 15 mins before dried at 80 °C for 30 mins furnishing the corresponding films with thicknesses of 24.5±0.9 μm.

Analytical and test methods

The characteristics of the nanomaterials were illustrated by using X-ray diffraction (XRD) on a Bruker D8 Advance and Scanning electron microscopy (SEM) on a Hitachi S-4800 microscope (Japan). The compositional analysis of prepared materials was performed using the Energy dispersive X-ray (EDX) on a 2100 HSX JEOL (Japan). Besides, the optical properties of prepared materials were determined using UV/Vis spectroscopy on a Cary UV-5000 spectrophotometer. Water contact angle (WCA) and gloss were determined on a Micro-TRI-Gloss (Germany), applying the standard measurement angle of 60 °. The color deviation was measured on a Chroma Meter CR-400 Konica Minolta INC (Japan). Mechanical strengthen was assessed using the DIN standards. The QUV accelerated weathering test (AWT) was carried out according to ASTM D4587 standard.

Results and discussion

Characterization of the nanocomposites

The crystal structures of CS NCs were characterized by XRD analysis (figure 1). As can be seen, typical peaks assigned to the cristobalite phase of SiO_2 were observed at 21.9°, 31.4°, and 36.1° (JCPDS no. 01-077-8627), which are at planes (101), (102), and (200), respectively [22,23]. In addition to SiO_2, XRD results clearly reveal peaks assigned to the cerianite phase of CeO_2. The peaks responsible for the CeO_2 cerianite phase were observed at 28.7°, 33.2°, 47.4°, and 56.1° or planes (111), (200), (220), and (311), respectively [24,25]. These peaks are ascribed to the face-centered cubic (fcc) crystal structure of cerianite with the Fm-3m space group (JCPDS no. 00-054-0593) [26]. The result pointed that CS NCs were successfully synthesized at a calcination temperature of 650 °C.

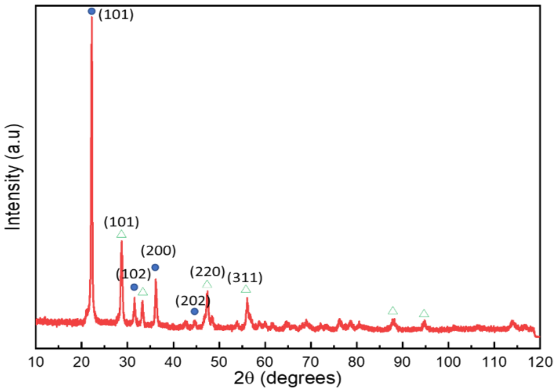

Figure. 1: The XRD pattern of the CS NCs prepared at 650 °C calcination temperature. In the figure, the circle (●) represents for SiO_2 phase while the triangle (△) represents for CeO_2 phase

The morphology of the nanocomposites was shown in figure 2 below. The measurement was performed by the Vietnam Academy of Science and Technology. Analysis results show that the CS NCs nanocomposites have a highly porous structure with an average pore size is about 50nm. The prepared materials were used directly in the preparation of PU thin films.

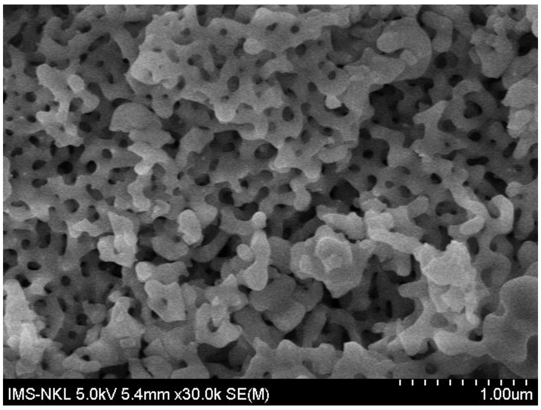

Figure 2: SEM image of CS NCs which calcined at 650 °C

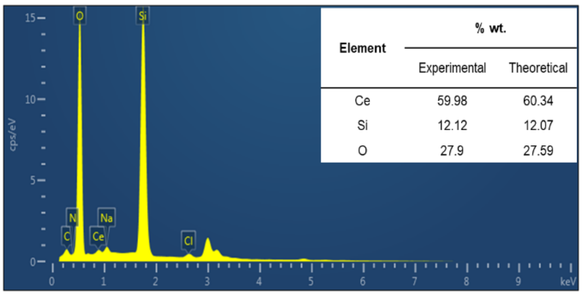

Element	% wt.	
	Experimental	Theoretical
Ce	59.98	60.34
Si	12.12	12.07
O	27.9	27.59

Figure 3: Compositional analysis of prepared CS NCs

According to the EDX compositional analysis, Ce, Si, and O atoms were presented similar to the theoretical calculation in the nanocomposites (figure 3). This implies the material was successfully synthesized.

Performance of CS NCs embedded PU thin films

Figure 4A shows SEM images of pure PU coating, whereas figure 4B corresponding to composites with 0.5 wt% contents of CS NCs. One may notice from figure 4A, the presence of CS NCs reduces fractures of the PU hybrid coatings. The coatings exhibited a much smoother structure with little evidence of microscopic cracks at any content of nanocomposites. Since the bonding force between PU is very weak, micro-cracks start to occur at the interface junction and continue to extend under the action of weathering pressures (i.e., oxygen, UV, temperature, water) [27]. The propagation of cracks results in cracking or delamination of the coating (figure 4A). When the coat has the presence of CS NCs, the strong interfacial interaction between CS NCs and PU could enhance the tensile strength. The interaction happens because the CS NCs have high surface polarity making it easy to form aggregation in the PU. However, adding too many CS NCs would cause it to agglomerate heavily in the PU, which leads to a decrease in tensile strength [17].

As clearly seen from Figure 4C and Figure 4D, after 700h of UV irradiation, a major surface changes of pure PU film occurred without the presence of CS NCs. On the other hand, with only 0.5 wt% of CS NCs, the change on the coating surface was relatively small.

The prepared coatings were named according to their content in the films 0 %, 0.1 %, 0.25 %, 0.5 %, 0.75 %, 1.0 %, 1.5 % and 2.0 % (i.e., **F0**, **F0.1**, **F0.25**, **F0.5**, **F0.75**, **F1.0**, **F1.5** and **F2.0**, respectively). Some mechanical properties of PU film with and without nanomaterials were presented in table 1.

From table 1, the physical properties of the polyurethane material system after dispersing the material were still maintained. The addition of an amount of material between 0.1 % and 2 % has no effect on the mechanical and physical properties of the material. This promises good applicability of the material in polyurethane substrates. Previous studies pointed out in some cases, the presence of nanomaterial, mechanical properties of the PU coating can be enhanced [28-30]. In addition, after 700 h of AWT, the films confirmed the same most of PU properties such as appearance, adhesion, flexural strength. Only pencil hardness is changing from HB to 3B for all materials. These results indicate that there is also a slight change in the hardness of the material after 700 h under the influence of the weather.

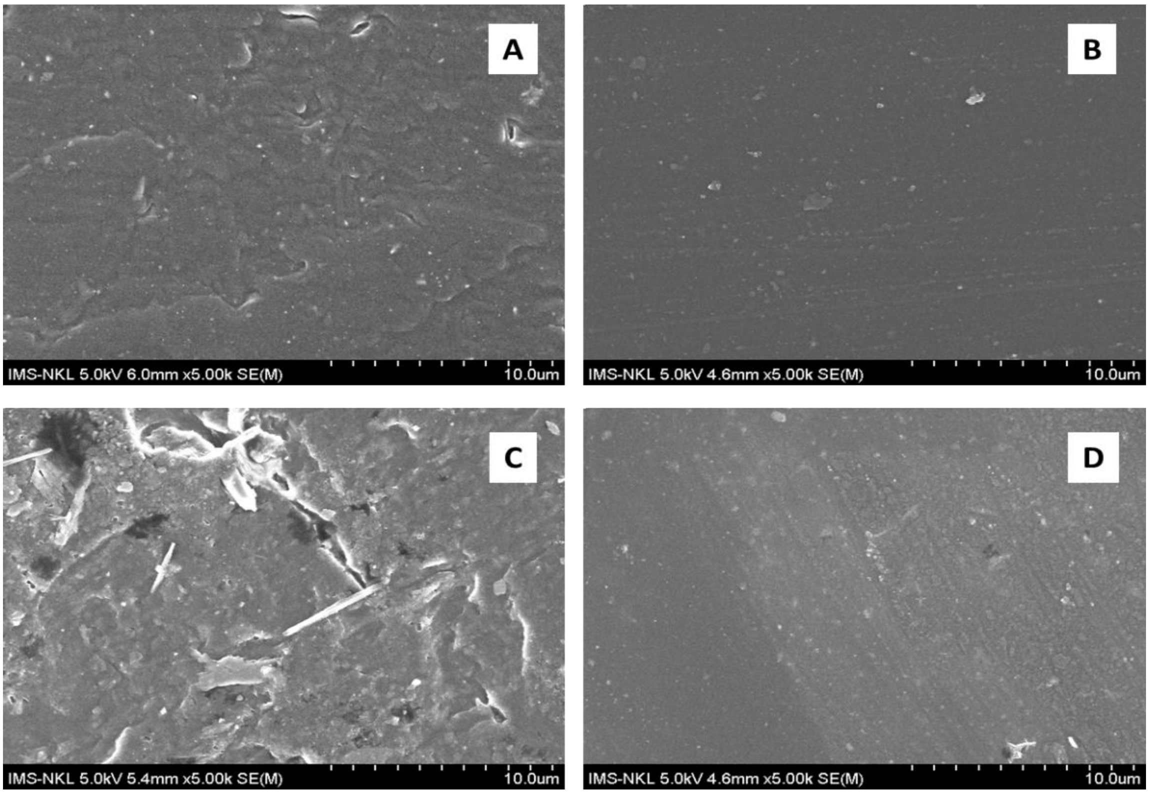

Figure 4: The SEM images of pure PU thin film (A), PU embedded with 0.5 wt% of CS NCs (B), pure PU thin film after 700h of UV irradiation (C), and PU embedded with CS NCs after 700h of UV irradiation (D).

Table 1: Some of the mechanical properties of PU films prior to being illuminated in the QUV testing according to BEVS 1601/3 Sheen standard.

Samples	Content of CS NCs in the PU films							
	0 %	0.1 %	0.25 %	0.5 %	0.75 %	1.0 %	1.5 %	2.0 %
Film-forming ability	Good	Good	Good	Good	Good	Good	Good	Good
Film appearances	Good	Good	Good	Good	Good	Good	Good	Good
Hardness*	HB	HB	HB	HB	HB	HB	HB	HB
Adhesion	100/100	100/100	100/100	100/100	100/100	100/100	100/100	100/100
Solvent resistance	100DR	100DR	100DR	100DR	100DR	100DR	100DR	100DR
Flexural strength	2T	2T	2T	2T	2T	2T	2T	2T

*The only parameter that changes after 700 h of accelerated weathering test, the value changes from HB to 3B for all content of CS NCs.

https://doi.org/10.51316/jca.2021.117

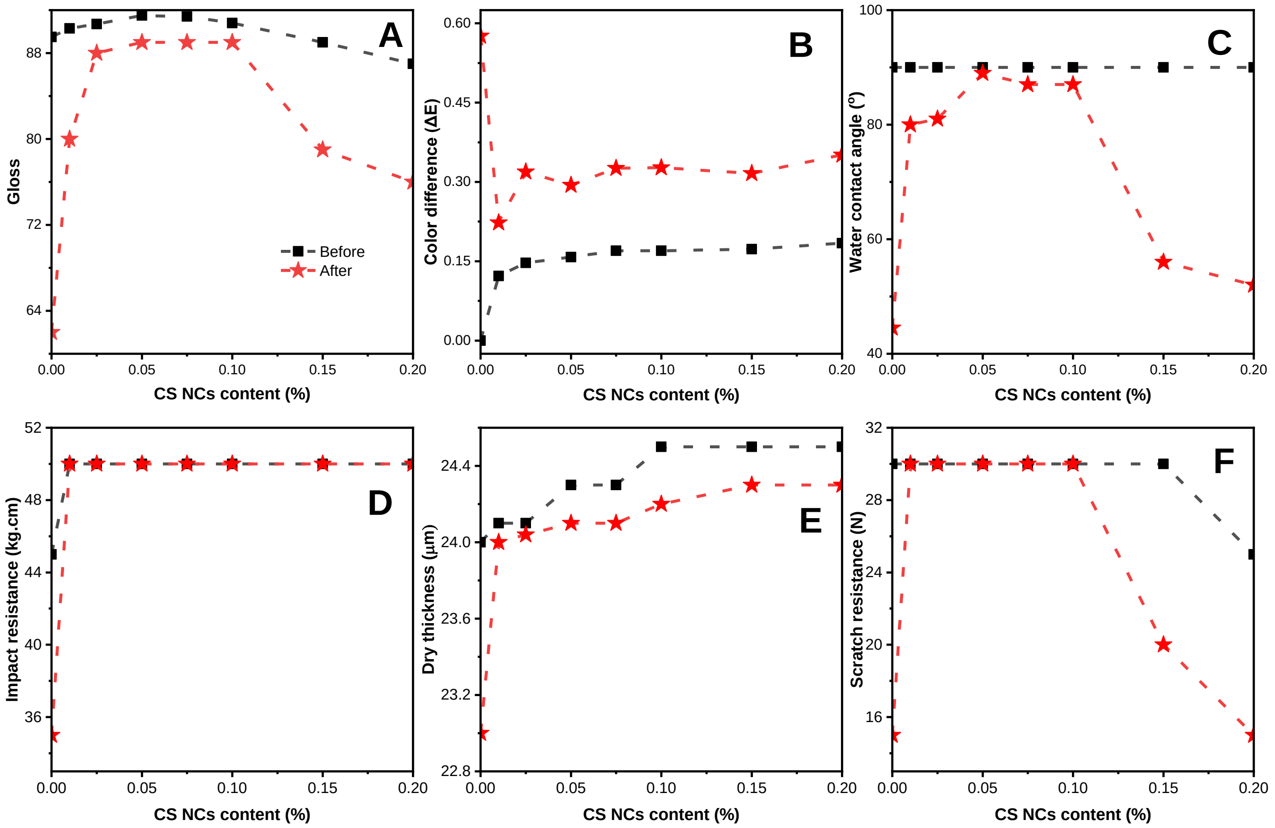

Figure 5: PU thin film's parameters before and after 700 h of the QUV accelerated weathering test A) Gloss B) Color difference C) Water contact angle D) Impact resistance E) Dry thickness E) Scratch resistance.

Besides, the mechanical properties, figure 5 shows other physical properties change after the weathering test, including color differences, water contact angle, impact resistance, dry thickness, scratch resistance, and gloss of the PU coatings embedded with different concentrations of CS-NCs.

Yang et al. explained that the loss of gloss increases along with the change of surface roughness which causes by the formation of surface damages.[31] figure 5A shows the gloss of PU films before and after subjecting to a 700h AWT. As we can see, before the AWT, the gloss is comparable for all PU films even though the CeO_2 itself has light yellow color because of the relatively small amount of the nanomaterial in the films.[11] Without the presence of CS NCs, the film degrades quickly, and failures happen inevitably. Similar observations are also illustrated in figure 5B, C, D, F for all other properties (i.e., color difference, water contact angle, impact resistance, and scratch resistance, respectively). However, the advantages of CS NCs only remain at a certain loading level. This conclusion can be pointed out from the loss of gross. For example, the blank PU film (i.e., **F0**) showed the fastest loss, followed by **F2.0** (figure 5A) or the water contact angle the **F0**, **F1.5**, and **F2.0** have comparable level of decreasing (figure 5C). The possible explanation for this might be related to the UV absorption capacity of the films. On one hand, the conventional PU films, under the weathering pressure (i.e., UV irradiation, water, temperature), ages rapidly. On the other hand, large amount of the nanomaterial can cause a high self-agglomeration. Besides, CS NCs also can produce electron-hole pair which reacts with water, oxygen to form free radicals. When the formed free radicals are over the capability of the film can relax, they make a fast degradation. This study result indicated that adsorption capacity linearly increases as the content of CS-NCs from 0.25 wt% to 1.0 wt% (i.e., **F0.25** and **F1.0**). The results of all properties well agreed with the statements.

One of the interesting results can be obtained from figure 5, which is about the color difference. The color of the polymer deviated gradually, which was caused by the slow deterioration of the film's surface [32]. Figure 5 indicates that PU films show an exceptional UV resistance against discoloration during AWT. For example, in 2009, Jalili and Moradian reported ΔE values of 2–4.8 for nano-silica embedded PU coats under 200 h of QUV weathering or more recently, Saadat-Monfared et al. said ΔE values of 1-1.2 for nano-ceria embedded PU coats in 700 h of weathering exposure [33,34]. This difference is a strong indicator of the efficiency of CS-NCs as a UV absorber in the PU coat.

Conclusion

To summarize, the dispersion of CS NCs materials in PU films using a simple, safe, and effective method was successfully reported. The incorporation of CS NCs in PU films introduces several beneficial impacts such as appearance, pencil hardness or adhesion. Those mechanical properties are not affected during the weathering test. Interestingly, the prepared PU films show a low value of color difference at all loading levels. Besides, the presence of CS NCs reduces the effect of UV irradiation on the roughness of the PU coating. Overall, the nanoparticle’s optimal concentration in the polyurethane film was in the range of 0.25-1.0 wt%.

Acknowledgments

This research is funded by the Vietnam Academy of Science and Technology (reference number TĐVLTT.01/21-23).

References

1. H.M.C.C. Somarathna, S.N. Raman, D. Mohotti, A.A. Mutalib, K.H. Badri., Constr. Build. Mater. 190 (2018) 995-1014. https://doi.org/10.1016/j.conbuildmat.2018.09.166
2. I. O. Oladele, T. F. Omotosho, A. A. Adediran., Int. J. Polym. Sci. (2020). https://doi.org/10.1155/2020/8834518
3. X. F. Yang, C. Vang, D. E. Tallman, G. P. Bierwagen, S.G. Croll, S. Rohlik., Polym. Degrad. Stab. 74 (2001) 341-351. https://doi.org/10.1016/S0141-3910(01)00166-5
4. J. F. Larché, P. O. Bussire, J. L. Gardette., Polym. Degrad. Stab. 95 (2010) 1810-1817. https://doi.org/10.1016/j.polymdegradstab.2010.05.005
5. T. T. Van, F. Abedin, A. Usta, R. Asmatulu., J. Compos. Mater. 53 (2019) 1387-1399. https://doi.org/10.1177/0021998318799402
6. T. Montini, M. Melchionna, M. Monai, P. Fornasiero., Chem. Rev. 116 (2016) 5987-6041. https://doi.org/10.1021/acs.chemrev.5b00603
7. F. Liu, A. Liu, W. Tao, Y. Yang., Prog. Org. Coatings. 145 (2020) 105685. https://doi.org/10.1016/j.porgcoat.2020.105685
8. I. Fajzulin, X. Zhu, M. Möller., J. Coatings Technol. Res. 12 (2015) 617-632. https://doi.org/10.1007/s11998-015-9683-2
9. N. N. Dao, M. D. Luu, Q. K. Nguyen, B. S. Kim., Adv. Nat. Sci. Nanosci. Nanotechnol. 2 (2011) 2-6. https://doi.org/10.1088/2043-6262/2/4/045013
10. A. Z. M. Rus, N. N. M. Hassan., Int. J. Polym. Sci. (2015). https://doi.org/10.1155/2015/615284
11. D.N. Nhiem, N.Q. Bac, D.T. Dung, P.N. Chuc, N.T.H. Chi, D.T. Lim., Adv. Mech. Eng., 10 (2018) 1-5. https://doi.org/10.1177/1687814018816770
12. F. Chen, D. Zhou, L. Yang, J. Sun, J. Wu., Mater. Res. Express. 6 (2019) 015308. https://doi.org/10.1088/2053-1591/aae636
13. G. Cai, S. Xiao, C. Deng, D. Jiang, X. Zhang, Z. Dong, Corros. Sci., 178 (2021) 109014. https://doi.org/10.1016/j.corsci.2020.109014
14. N. N. Dao, T. H. C. Nguyen, T. D. Doan, N. C. Pham, Q. B. Nguyen, T. L. Duong, N. N. Pham, V. N. M. Nguyen. J. Polym. Res. 28 (2021) 1-11. https://doi.org/10.1007/s10965-021-02487-0
15. E. J. S. Christy, R. Alagar, M. Dhanu, A. Pius., Environ. Nanotechnol., Monit. Manag. 14 (2020) 100365. https://doi.org/10.1016/j.enmm.2020.100365
16. N. V. N. Mai, D. T. Lim, N. Q. Bac, N. T. H. Chi, D. T. Dung, N. N. Pham, D. N. Nhiem., J. Chinese Chem. Soc. 67 (2020) 242-245. https://doi.org/10.1002/jccs.201900033
17. H. Wang, W. Lin, X. Qiu, F. Fu, R. Zhong, W. Liu, D. Yang., ACS Sustain. Chem. Eng. 6 (2018) 3696-3705. https://doi.org/10.1021/acssuschemeng.7b04038
18. J. Lin, Y. Wu, A. Khayambashi, X. Wang, Y. Wei. Adsorpt. Sci. Technol. 36 (2018) 743-761. https://doi.org/10.1021/acssuschemeng.7b04038
19. B.M. Reddy, A. Khan, P. Lakshmanan, M. Aouine, S. Loridant, J.C. Volta, J. Phys. Chem. B. 109 (2005) 3355-3363. https://doi.org/10.1021/jp045193h
20. M. Ari, K. J. Miller, B. A. Marinkovic, P. M. Jardim, R. de Avillez, F. Rizzo, M. A. White. J. Sol-Gel Sci. Technol. 58 (2011) 121-125. https://doi.org/10.1007/s10971-010-2364-9
21. A. R. Bueno, R. F. M. Oman, P. M. Jardim, N. A. Rey, R. R. De Avillez. Microporous Mesoporous Mater. 185 (2014) 86-91. https://doi.org/10.1016/j.micromeso.2013.10.021

22. P. Bruhns, R. X. Fischer, Eur. J. Mineral. 12 (2000) 615-624. https://doi.org/10.1127/0935-1221/2000/0012-0615
23. Y. Shinohara, N. Kohyama, Ind. Health. 42 (2004) 277-285. https://doi.org/10.2486/indhealth.42.277
24. J. Li, Y. Hao, H. Li, M. Xia, X. Sun, L. Wang. Microporous Mesoporous Mater. 12i0 (2009) 421-425. https://doi.org/10.1016/j.micromeso.2008.12.014
25. F.Wang, K. Wang, Y. Muhammad, Y. Wei, L. Shao, X. Wang. ACS Sustain. Chem. Eng. 7 (2019) 14716–14726. https://doi.org/10.1021/acssuschemeng.9b02643
26. E. Poonia, P. K. Mishra, V. Kiran, J. Sangwan, R. Kumar, P. K. Rai, R. Malik, V. K. Tomer, R. Ahuja, Y. K. Mishra, J. Mater. Chem. C 7 (2019) 5477-5487. https://doi.org/10.1039/C9TC01081E
27. T. Bai, L. Lv, W. Du, W. Fang, Y. Wang, Nanomaterials 10 (2020) 137. https://doi.org/10.3390/nano10010137
28. R. Rodríguez, B. Pérez, S. Flórez, J. Adhes. 90 (2014) 848-859. https://doi.org/10.1080/00218464.2014.893509
29. H. He, K. Li, J. Wang, G. Sun, Y. Li, J. Wang, Mater. Des. 32 (2011) 4521-4527. https://doi.org/10.1016/j.matdes.2011.03.026
30. S. H. Lee, C. R. Oh, D. S. Lee, Nanomaterials 9 (2019) 1-5. https://doi.org/10.3390/nano9030389
31. X. F. Yang, D. E. Tallman, G.P. Bierwagen, S.G. Croll, S. Rohlik, Polym. Degrad. Stab. 77 (2002) 103-109. https://doi.org/10.1016/S0141-3910(02)00085-X
32. J. Liu, Z. Li, L. Zhang, J. Hou, Z. Lu, P. Zhang, B. Wang, N. Jin, Prog. Org. Coatings 136 (2019) 105310. https://doi.org/10.1016/j.porgcoat.2019.105310
33. M.M. Jalili, S. Moradian, Prog. Org. Coatings 66 (2009) 359-366. https://doi.org/10.1016/j.porgcoat.2009.07.011
34. A. Saadat-Monfared, M. Mohseni, M. H. Tabatabaei, Colloids Surfaces A Physicochem. Eng. Asp. 408 (2012) 64-70. https://doi.org/10.1016/j.colsurfa.2012.05.027